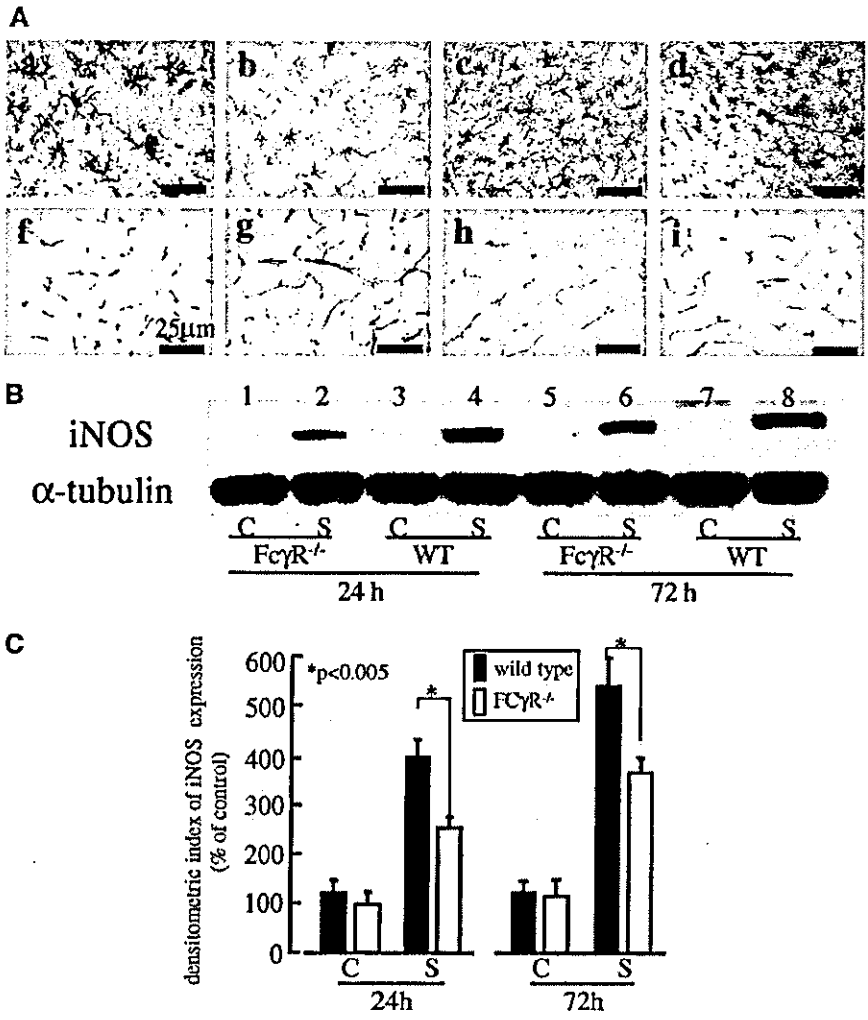


Figure 4. A, Photomicrographs show iNOS staining in representative WT and FcγR$^{-/-}$ mice. Shown are WT mice (a to d) and FcγR$^{-/-}$ mice (e to h) 24 hours (a, e), 48 hours (b, f), 72 hours (c, g), and 7 days (d, h) after reperfusion. In WT mice, many iNOS-positive cells were detected in microglia in the transition area, while iNOS immunoreactivity was observed only in the endothelial cells in the ischemic core of FcγR$^{-/-}$ mice. Magnification ×200. B, Western blot analysis of iNOS. The samples were prepared from the brain at 24 hours (FcγR$^{-/-}$ mice: lanes 1 and 2; WT mice: lanes 3 and 4) and 72 hours (FcγR$^{-/-}$ mice: lanes 5 and 6; WT mice: lanes 7 and 8) after reperfusion. With the use of iNOS antibody, a 130-kDa band was detected on the stroke side. The intensity of the specific band increased in a time-dependent manner. FcγR$^{-/-}$ mice showed less intensity of the band. C, Densitometric analysis. Values are expressed as percentage of control. C indicates contralateral lesion; S, stroke side.

compared with WT mice (Figure 3Aa to 3Af, 3B). Immunoblots of Iba-1 were clearly detected in the ischemic lesion as a protein band at 17 kDa. In WT mice, the intensity of the band increased in the stroke side ($P<0.002$) in a time-dependent manner compared with FcγR$^{-/-}$ mice (Figure 3C, 3D).

### Induction of iNOS in FcγR$^{-/-}$ Mice

In WT mice, induction of iNOS in microglia of the peri-ischemic area reached a peak level at 48 to 72 hours after reperfusion (Figure 4Ab, 4Ac). On the other hand, in FcγR$^{-/-}$ mice, iNOS was detected only in endothelial cells of the ischemic core area (Figure 4Ae to 4Ah). Immunoblots of iNOS were detected as a protein band at 130 kDa. In WT mice, the intensity of the iNOS band in the stroke side was stronger ($P<0.005$) than the corresponding site in FcγR$^{-/-}$ littermates (Figure 4B, 4C).

### Activation of Bone Marrow–Derived Macrophages in FcγR$^{-/-}$ Mice

At 7 days after reperfusion, double immunostaining for EGFP and Iba-1 showed many morphologically phagocytic EGFP/Iba-1–positive cells in the ischemic core and many amoeboid-like EGFP/Iba-1–positive cells in the transition area of WT/EGFP chimera mice. These findings indicated activation and migration of EGFP-positive bone marrow–derived microglia/macrophages in WT/EGFP chimera mice (Figure 5b, 5c). In contrast, microglial staining was comparatively less in FcγR$^{-/-}$/EGFP chimera mice (Figure 5e, 5f), and only a few ramified Iba-1/EGFP–positive cells with branching processes were detected in the transitional area. In WT/EGFP chimera mice, some EGFP/iNOS-positive cells were detected in the transition area, but many EGFP-positive intrinsic microglia did not exhibit iNOS and were observed in endothelial cells (Figure 5g, 5h). On the other hand, iNOS staining was detected only in endothelial cells in the FcγR$^{-/-}$/EGFP chimera mice (data not shown). In WT/EGFP chimera mice, induction of nitrotyrosine in microglia of the transition area was detected (Figure 5i), and nitrotyrosine staining was observed in the luminal surface of vessels at ischemic lesions (Figure 5j), while there were few nitrotyrosine-positive cells in FcγR$^{-/-}$/EGFP chimera mice (data not shown). These nitrotyrosine-positive microglia did not stain for EGFP.

## Discussion

In the present study we analyzed the effects of brain ischemia on the functional contribution of FcγR by using FcγR$^{-/-}$ mice. The major finding of the present study was that FcγR$^{-/-}$ mice were protected from progression and expansion of infarct volume after focal cerebral ischemia followed by reperfusion.

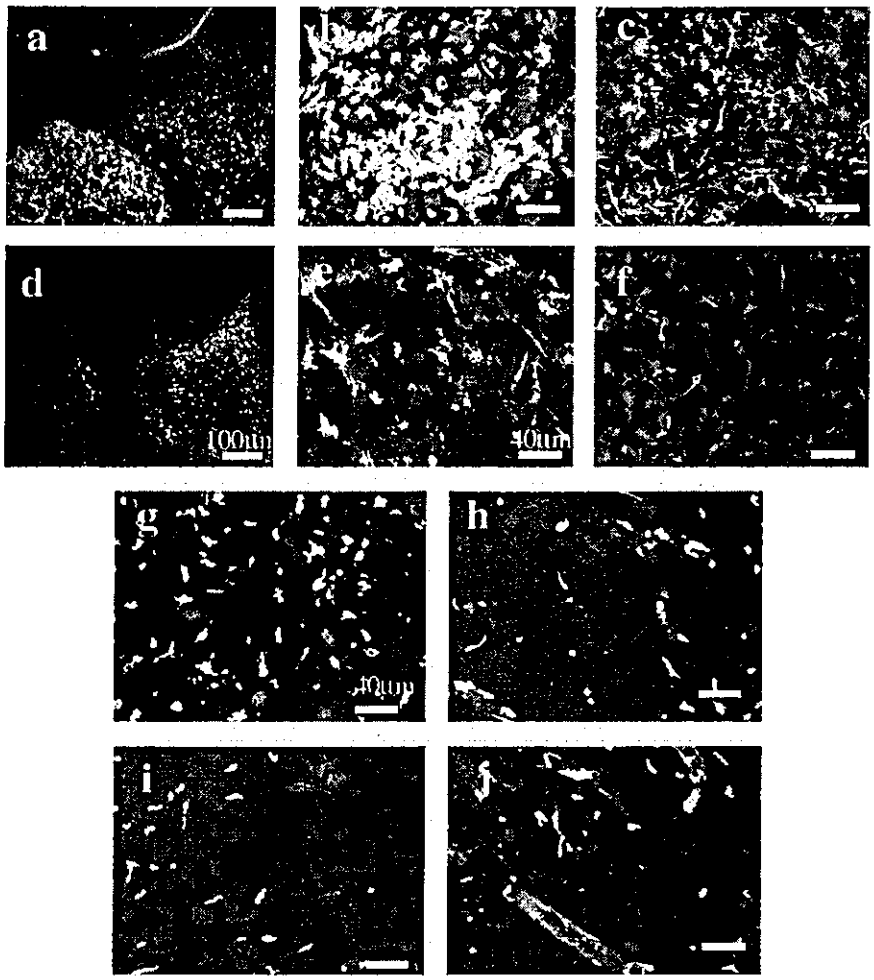


**Figure 5.** Photomicrographs show double-immunofluorescence labeling of WT/EGFP (a to c, g to j) and FcγR$^{-/-}$/EGFP chimera mouse (d to f) brain. Shown are 7 days (a to f) and 72 hours (g to j) after reperfusion at the ischemic core (b, e) and transition area (c, f to j). a to f, Iba-1–stained cells appear red in color. EGFP/Iba-1–positive cells are seen in these areas. Many irregularly shaped EGFP/Iba-1–positive cells and some with processes are seen in WT/EGFP chimera mice (a to c), while fewer cells are detected in FcγR$^{-/-}$/EGFP littermates (d to f). g, h, iNOS/EGFP double-immunofluorescence staining of WT/EGFP chimera mouse. i, j, Nitrotyrosine/EGFP double-immunofluorescence staining of WT/EGFP chimera mouse. Magnification ×100 for a and d; magnification ×400 for b, c, e to j.

To our knowledge, there are no studies that proposed the involvement of a FcγR-dependent pathway in the pathogenesis of cerebral ischemia/reperfusion injury. FcγR promotes phagocytosis, antibody-dependent cell-mediated cytotoxicity, activation of inflammatory cells, and antibody-dependent immunity.[12] In the present study, using FcγR$^{-/-}$ mice, we demonstrated that FcγR contributed to the activation of microglia, induction of iNOS followed by generation of reactive oxygen species, and infiltration of bone marrow–derived macrophages during cerebral ischemia/reperfusion. To our knowledge, this is the first report on the functional role of FcγR on microglia/macrophages in cerebral ischemia/reperfusion injury.

Cerebral ischemia/reperfusion injury is associated with the development of inflammatory response, including pathological contributions from vascular leukocytes and endogenous microglia.[2] In the ischemic brain, microglia/macrophages are the major source of inflammatory cytokines.[1,13] Therefore, inhibition of microglial activation can protect against stroke-associated pathological changes.[14] After ischemia, microglial activation results in a series of functional and morphological modifications that involve proliferation.[15] The present results showed that microglial activation was markedly suppressed in ischemic lesions from the early stage of reperfusion in FcγR$^{-/-}$ mice compared with WT mice. Our results provide strong evidence that FcγR plays a crucial role in the initiation and progression of neuronal damage by activation and proliferation of microglia.

In WT mice, iNOS immunoreactivity was observed in activated microglia and reached a peak level at 48 to 72 hours after reperfusion. However, in FcγR$^{-/-}$ mice, iNOS immunoreactivity was not detected in microglia but only in endothelial cells. In addition, iNOS-positive microglia and nitrotyrosine-positive microglia were observed in WT/EGFP chimera mice but not in FcγR$^{-/-}$/EGFP littermates. In our bone marrow transplantation model, induction of iNOS does not occur on the invading macrophages. Therefore, the possible mechanisms involved in the reduction of infarction volume during brain ischemia/reperfusion include the suppression of activation of microglia followed by induction of iNOS and peroxynitrite production through the FcγR-dependent pathway. In contrast to neuronal NOS, which generates NO early after onset of ischemia,[16] iNOS appears somewhat later in inflammatory cells and contributes to the evolution of brain injury. Furthermore, suppression of iNOS expression has been demonstrated to play a major role as a protective agent in several experimental models, such as iNOS null mice,[16,17] treatment with antisense oligodeoxynucleotide to iNOS,[18] administration of iNOS inhibitors,[19] and mild hypothermia.[20] In the present study, therefore, it is possible that the potential neuroprotective role of the FcγR-dependent pathway is mediated in part by the suppression of

iNOS upregulation and peroxynitrite production in activated microglia.

In our bone marrow transplantation model, although FcγR was present in the donor EGFP-positive cells, activation and migration of EGFP-positive bone marrow–derived macrophages were markedly reduced in $Fc\gamma R^{-/-}$ mice compared with WT mice. Microglial activation has been observed as early as 6 hours after insult,[21] followed by subsequent macrophage transmigration. A previous study reported that reactive microglia showed increased expression of FcRs and that engagement of FcγR triggered inflammatory, cytolytic, or phagocytic activities.[22] The mechanism of migration and infiltration of bone marrow–derived cells into infarcted areas is a topic of debate and remains unclear but may involve the FcγR-dependent pathway for macrophages or some activating signals from activated microglia. Taken together, our results indicate that the signaling pathway through the FcγR on residual microglia may play an important role in the migration and activation of bone marrow–derived macrophages.

In this study we demonstrated that FcγR deficiency decreased the inflammatory responses through microglial activation, iNOS induction, and bone marrow–derived macrophage infiltration after transient focal cerebral ischemia/reperfusion. Therefore, the neuroprotective effect of FcγR deficiency may be primarily attributable to suppression of inflammatory cell activation and infiltration. Our data showed that anti-inflammatory therapy through the FcγR may be useful for neuroprotection after cerebral infarction. Suppression of the FcγR-dependent pathway may provide an approach to potentially reduce ongoing damage during reperfusion in stroke patients.

## Acknowledgments

This study was supported in part by a High Technology Research Center grant and a grant-in-aid for exploratory research from the Ministry of Education, Culture, Sports, Science, and Technology, Japan. The anti–Iba-1 polyclonal antibody was a kind gift from Y. Imai and S. Kohsaka from the Department of Neurochemistry, National Institute of Neuroscience, Tokyo, Japan.

## References

1. Davies CA, Loddick SA, Toulmond S, Stroemer RP, Hunt J, Rothwell NJ. The progression and topographic distribution of interleukin-1beta expression after permanent middle cerebral artery occlusion in the rat. *J Cereb Blood Flow Metab.* 1999;19:87–98.
2. Clark RK, Lee EV, White RF, Jonak ZL, Feuerstein GZ, Barone FC. Reperfusion following focal stroke hastens inflammation and resolution of ischemic injured tissue. *Brain Res Bull.* 1994;35:387–392.
3. Ravetch JV. Fc receptors: rubor redux. *Cell.* 1994;78:553–560.
4. Sylvestre DL, Ravetch JV. Fc receptors initiate the Arthus reaction: redefining the inflammatory cascade. *Science.* 1994;265:1095–1098.
5. Abdul-Majid K-B, Stefferl A, Bourquin C, Lassmann H, Linington C, Olsson T, Kleinau S, Harris RA. Fc receptors are critical for autoimmune inflammatory damage to the central nervous system in experimental autoimmune encephalomyelitis. *Scand J Immunol.* 2002;55:70–81.
6. He Y, Le WD, Appel SH. Role of Fc receptors in nigral cell injury induced by Parkinson disease immunoglobulin injection into mouse substantia nigra. *Exp Neurol.* 2002;176:322–327.
7. Tanaka R, Komine-Kobayashi M, Mochizuki M, Yamada M, Furuya T, Migita M, Shimada T, Mizuno Y, Urabe T. Migration of enhanced green fluorescent protein expressing bone marrow-derived microglia/macrophage into the mouse brain following permanent focal ischemia. *Neuroscience.* 2003;117:531–539.
8. Suzuki Y, Shirato I, Okumura K, Ravetch JV, Takai T, Tomino Y, Ra C. Distinct contribution of Fc receptors and angiotensin II-dependent pathways in anti-GBM glomerulonephritis. *Kidney Int.* 1998;54:1166–1174.
9. Hara H, Huang PL, Panahian N, Fishman MC, Moskowitz MA. Reduced brain edema and infarction volume in mice lacking the neuronal isoform of nitric oxide synthase after transient MCA occlusion. *J Cereb Blood Flow Metab.* 1996;16:605–611.
10. Lin TN, He YY, Wu G, Khan M, Hsu CY. Effect of brain edema on infarct volume in a focal cerebral ischemia model in rats. *Stroke.* 1993;24:117–121.
11. Ito D, Imai Y, Ohsawa K, Nakajima K, Fukuuchi Y, Kohsaka S. Microglia-specific localisation of a novel calcium binding protein, Iba1. *Mol Brain Res.* 1998;57:1–9.
12. Ravetch JV, Kinet JP. Fc receptors. *Annu Rev Immunol.* 1991;9:457–492.
13. Lambertsen K, Gregersen R, Finsen B. Microglial-macrophage synthesis of tumor necrosis factor after focal cerebral ischemia in mice is strain dependent. *J Cereb Blood Flow Metab.* 2000;20:53–65.
14. Yrjanheikki J, Tikka T, Keinanen R, Goldsteins G, Chan PH, Koistinaho J. A tetracycline derivative, minocycline, reduces inflammation and protects against focal cerebral ischemia with a wide therapeutic window. *Proc Natl Acad Sci U S A.* 1999;96:13496–13500.
15. Kato H. The role of microglia in ischemic brain injury. In: Feurstein GZ, ed. *Inflammation and Stroke.* Boston: Birkhauser Verlag, 2001;89–99.
16. Iadecola C. Bright and dark sides of nitric oxide in ischemic brain injury. *Trends Neurosci.* 1997;20:132–139.
17. Zhao X, Haensel C, Araki E, Ross ME, Iadecola C. Gene-dosing effect and persistence of reduction in ischemic brain injury in mice lacking inducible nitric oxide synthase. *Brain Res.* 2000;872:215–218.
18. Parmentier-Batteur S, Bohme GA, Lerouet D, Zhou-Ding L, Beray V, Margaill I, Plotkine M. Antisense oligodeoxynucleotide to inducible nitric oxide synthase protects against transient focal cerebral ischemia-induced brain injury. *J Cereb Blood Flow Metab.* 2001;21:15–21.
19. Nagayama M, Zhang F, Iadecola C. Delayed treatment with aminoguanidine decreases focal cerebral ischemic damage and enhances neurological recovery in rats. *J Cereb Blood Flow Metab.* 1998;18:1107–1113.
20. Han HS, Qiao Y, Karabiyikoglu M, Giffard RG, Yenari MA. Influence of mild hypothermia on inducible nitric oxide synthase expression and reactive nitrogen production in experimental stroke and inflammation. *J Neurosci.* 2002;22:3921–3928.
21. Lyons SA, Pastor A, Ohlemeyer C, Kann O, Wiegand F, Prass K, Knapp F, Kettenmann H, Dirnagl U. Distinct physiologic properties of microglia and blood-borne cells in rat brain slices after permanent middle cerebral artery occlusion. *J Cereb Blood Flow Metab.* 2000;20:1537–1549.
22. Ulvestad E, Williams K, Vedeler C, Antel J, Nyland H, Mørk M, Matre R. Reactive microglia in multiple sclerosis lesions have an increased expression of receptors for the Fc part of IgG. *J Neurol Sci.* 1994;121:125–131.

Journal of Dermatological Science (2004) 34, 54–55

ELSEVIER

Journal of Dermatological SCIENCE

www.intl.elsevierhealth.com/journals/jods

LETTER TO THE EDITOR

## Expression of phosphorylated Smad2 in normal human epidermis

Transforming growth factor-β (TGF-β) is a multifunctional cytokine that plays an important role in the regulation of cell growth, differentiation, apoptosis, and extracellular matrix production in a variety of cell types [1]. In the skin, abundant expression of three mammalian isoforms of TGF-βs (TGF-β1, -β2, -β3) are demonstrated at mRNA and protein levels in human epidermis by using in situ hybridization technique or immunohistochemistry [2–4] and it has been implicated in growth regulation of keratinocytes based on the evidence that (1) TGF-βs inhibit proliferation of normal human keratinocytes in vitro [5] and (2) transgenic mice that overexpress dominant negative TGF-β type II receptor in the epidermis show hyperplastic epidermis with increased BrdU uptake in basal and suprabasal keratinocytes [6].

However, elucidating functional significance of TGF-β expression in the skin has been hampered by the fact that TGF-β is produced and secreted by cells in a latent form, which must then be activated before interaction with TGF-β receptors on the cell surface [7]. Mere elevation of TGF-β mRNA or protein expression is therefore not automatically an indication that active TGF-β is being produced. Thus, even though several papers reported TGF-β mRNA or protein expression in normal and pathological states of human epidermis, it might not be an accurate reflection of active TGF-β secretion in the human epidermis.

Therefore, to determine whether human epidermis indeed received signals of TGF-β, we examined expression of phosphorylated Smad2 in normal human skin by immunohistochemical study using an antibody specifically recognized phosphorylated Smad2. Recent studies have revealed that TGF-β1, -β2, -β3 bind to the cell surface TGF-β type I and type II receptors and the ligand-bound activated TGF-β receptor complex phosphorylate cytoplasmic Smad2 and Smad3, which form hetero-trimeric complex with Smad4, respectively, and enter the nucleus, bind directly or indirectly to DNA, and regulate transcription of many TGF-β target genes in cooperation with various transcriptional factors [8]. Thus, phosphorylation of Smad2 or Smad3 is a key event for initiation of TGF-β signalling.

Normal skin samples were obtained from subjects undergoing plastic surgery ($n = 6$) after written informed consent. As shown in Fig. 1, we found that expression of phosphorylated Smad2 was prominent in the nucleus of keratinocytes in whole epidermis of the skin specimen. Similar finding was observed in all the normal skin specimens from six subjects. The exclusive nuclear staining of phosphorylated Smad2 indicated that Smad2 was activated by TGF-β receptors and translocated to the nucleus in keratinocytes. Thus, the data suggested that normal human epidermis received signals of TGF-β in vivo.

As a comparison, we performed tunnel staining in normal human epidermis because terminal differentiation of normal human keratinocytes might be associated with enhanced cellular TGF-β and apoptotic cell death [9]. We asked whether phosphorylated Smad2-positive cells were parallel with keratinocytes undergoing apoptosis. As shown in Fig. 2, TUNEL positive cells in the epidermis were largely detected at the granular layer in the epidermis, which was different from the expression pattern of phosphorylated Smad2. The results may suggest that activation of TGF-β/Smad2 signalling is not relevant to induction of keratinocyte apoptosis in vivo because phosphorylation of Smad2 is observed in basal and suprabasal keratinocytes which are not committed to apoptosis. However, of course, more thorough investigation is required to prove that activation of TGF-β/Smad2 signalling is not involved in apoptotic cell death in human epidermis.

In conclusion, human epidermis receives signals of TGF-β, that is constitutively synthesised by epidermal keratinocytes as shown by many previous reports. It should be determined in future whether signalling pathways downstream of TGF-β/Smad2 is active or not and what physiological functions the TGF-β/Smad2 pathway mediates in human epidermis. Most importantly, how Smad2 activation occurs (how conversion of latent form of TGF-β to its active form occurs) in normal human epidermis remains to be elucidated.


doi:10.1016/j.jdermsci.2003.10.004

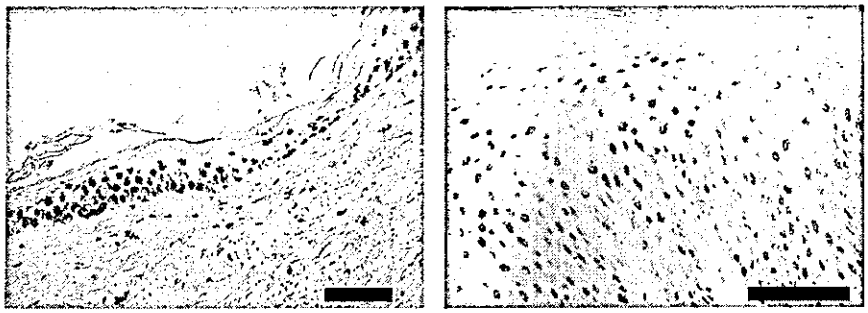

**Fig. 1** Expression of phosphorylated Smad2 in normal human epidermis. Four micrometer of cryostat sections of normal skin samples obtained from subjects undergoing plastic surgery were incubated with rabbit polyclonal antibody against phosphorylated Smad2 (#3101, Cell Signaling Technology Inc., Beverly, MA, USA) and then incubated with a biotinylated goat anti-rabbit antibody (1/200). Sections were then incubated with avidin biotin peroxidase complex (1/500) and 3-amino-9-ethyl carbazole (Sigma) was used as chromogen. Between steps, the slides were rinsed in Tris-buffered saline with 0.1% Triton X-100. All sections were lightly counterstained with hematoxylin. Positive cells were stained as brown in the nucleus. Scale bars represent 50 μm.

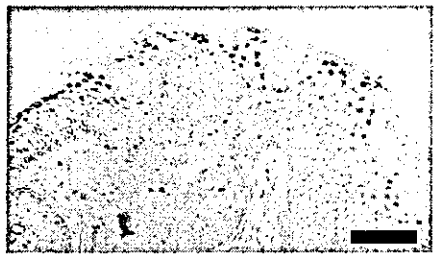

**Fig. 2** TUNEL staining in normal human epidermis. In situ detection of DNA fragmentation of the skin specimens obtained as described above was performed using terminal deoxynucleotidyltransferase-mediated dUTP nick-end labeling (TUNEL) staining using in situ tunnel staining kit (Takara Corp., Japan) according to the manufacturer's recommendation. Positive cells were stained as brown in the nucleus. Scale bars represent 50 μm.

## References


[1] Roberts AB, Sporn MB. Physiological actions and clinical applications of transforming growth factor-beta (TGF-beta). Growth Factors 1993;8:1–9.

[2] Kane CJ, Knapp AM, Mansbridge JN, Hanawalt PC. Transforming growth factor-beta 1 localization in normal and psoriatic epidermal keratinocytes in situ. J Cell Physiol 1990;144:144–50.

[3] Schmid P, Cox D, Bilbe G, McMaster G, Morrison C, Stahelin H, et al. TGF-betas and TGF-beta type II receptor in human epidermis: differential expression in acute and chronic skin wounds. J Pathol 1993;171:191–7.

[4] Quan T, He TY, John SK, Voorhees JJ, Fisher GJ. Ultraviolet irradiation alters transforming growth factor-β/Smad pathway in human skin in vivo. J Invest Dermatol 2002;119:499–506.

[5] Moses HL, Yang EY, Pietenpol JA. Regulation of epithelial proliferation by TGF-β. Ciba Found Symp 1991;157:66–74.

[6] Wang XJ, Greenhalgh DA, Bickenbach JR, Jiang A, Bundman DS, Krieg T, et al. Expression of a dominant-negative type II transforming growth factor beta (TGF-beta) receptor in the epidermis of transgenic mice blocks TGF-beta-mediated growth inhibition. Proc Natl Acad Sci USA 1997;94:2386–91.

[7] Miyazono K, Hellman U, Wernstedt C, Heldin CH. Latent high molecular weight complex of transforming growth factor-β. J Biol Chem 1988;263:6407–15.

[8] Massague J. How cells read TGF-β signals. Nature Rev Mol Cell Biol 2000;1:169–78.

[9] Min BM, Woo KM, Lee G, Park NH. Terminal differentiation of normal human oral keratinocytes is associated with enhanced cellular TGF-β and phospholipase C-γ1 levels and apoptotic cell death. Exp Cell Res 1999;249:377–85.



Meethong Prapars
Atsuhito Nakao*
Nobuhiro Nakano
Long Jin
Hideoki Ogawa
*Department of Dermatology, Atopy Research Center, Juntendo University School of Medicine 2-1-1 Hongo, Bunkyo-ku, Tokyo 113-8421, Japan*
*Corresponding author. Present address Department of Immunology, Faculty of Medicine University of Yamanashi, 1110 Shimokato, Tamaho Yamanashi 409-3898, Japan
Tel.: +81-55-273-6752; fax: +81-55-273-9542
*E-mail address:* anakao@yamanashi.ac.jp
(A. Nakao)

Microbiol. Immunol., 48(10), 755–759, 2004

# Genotype Analysis of *Malassezia restricta* as the Major Cutaneous Flora in Patients with Atopic Dermatitis and Healthy Subjects

**Takashi Sugita*[,1], Mami Tajima[2], Misato Amaya[2], Ryoji Tsuboi[2], and Akemi Nishikawa[3]**

[1]*Department of Microbiology and* [3]*Department of Immunobiology, Meiji Pharmaceutical University, Kiyose, Tokyo 204–8588, Japan, and* [2]*Department of Dermatology, Tokyo Medical University, Shinjuku-ku, Tokyo 160–0023, Japan*

Received May 18, 2004; in revised form, June 29, 2004. Accepted July 6, 2004

***Abstract*: Lipophilic yeasts of the genus *Malassezia* colonize the skin surface of humans and are an exacerbating factor in atopic dermatitis (AD). Two species, *M. restricta* and *M. globosa* are major cutaneous microflora in both AD patients and healthy subjects. We compared the DNA sequences of the intergenic spacer (IGS) region, located between the 26S and 5S rRNA genes of *M. restricta* colonizing the skin surfaces of 13 AD patients and 12 healthy subjects, and of three CBS stock strains as references. The IGS 1 sequences were divided into two major groups, corresponding to AD patients and healthy subjects. These findings suggest that a specific genotype of *M. restricta* plays a significant role in AD, although *M. restricta* commonly colonizes both AD patients and healthy subjects.**

***Key words*: *Malassezia restricta*, Atopic dermatitis, Cutaneous microflora, Genotype, IGS**

Lipophilic yeasts in the genus *Malassezia* are part of the normal human cutaneous microflora and are isolated from sebaceous-rich areas, particularly the chest, back, and head. They are a causative factor in *pityriasis versicolor* and seborrheic dermatitis (1, 4). In addition, *Malassezia* species are also thought to exacerbate atopic dermatitis (AD), based on findings that AD patients have specific serum IgE antibodies to *Malassezia* (11, 21, 22). Application of topical antifungal agents by AD patients decreases *Malassezia* colonization and the severity of eczematous lesions (2), suggesting that *Malassezia* species play a role in AD. We have analyzed the cutaneous *Malassezia* microflora of AD patients and healthy subjects using a non-culture method (nested PCR) (16). While *M. restricta* and *M. globosa* were detected in approximately 90% of the AD patients, other *Malassezia* species were found in fewer than 40%. In addition, we analyzed the DNA sequence divergence of the IGS region, which is located between the 26S and 5S rRNA genes of *M. globosa*, and found that the IGS sequence of *M. globosa* from AD patients differed from that from healthy subjects (19). These findings suggest that a specific genotype of this microorganism plays a significant role in AD.

**Address correspondence to* Dr. Takashi Sugita, Department of Microbiology, Meiji Pharmaceutical University, 2–522–1 Noshio, Kiyose, Tokyo 204–8588, Japan. Fax: +81–424–95–8762. E-mail: sugita@my-pharm.ac.jp

This paper describes the genotype of one of the major *Malassezia* microflora species, *M. restricta*, obtained from the skin of AD patients and healthy subjects.

## Materials and Methods

*Direct DNA sequencing of the IGS 1 region of* M. restricta *stock strains.* Three stock strains obtained from the Centraalbureau voor Schimmelcultures (Utrecht, The Netherlands) were analyzed: CBS 7877 (type strain of *M. restricta*), CBS 7991, and CBS 8747. The first two were isolated from the skin of a healthy subject in the UK, and the third was from the scalp of a healthy subject in Canada (http://www.cbs.knaw.nl/). Genomic DNA was extracted using the method of Makimura et al. (12). The IGS region containing 5S rDNA was amplified from each strain using the primer pair 26SBF (5'-AGCTGCTGCCAATGCTAGCTC) and Mala-R (5'-TACTGCTGTGAATGCTCCAGC) (18). The PCR products were sequenced using an ABI 310 DNA sequencer and a BigDye Terminator Cycle Sequencing Ready Reaction kit version 3.1 (Perkin-Elmer Applied Biosystems, Calif., U.S.A.) according to the manufacturer's instructions.

*Abbreviations*: AD, atopic dermatitis; CBS, Centraalbureau voor Schimmelcultures; IGS, intergenic spacer.

*Subjects.* Thirteen AD outpatients (9 males, 4 females; aged 20 to 64 years, mean age 33.9±11.3 years) at Tokyo Medical University Hospital and 12 healthy students (3 males, 9 females; aged 19 to 23 years, mean age 20.7±1.5 years) at Meiji Pharmaceutical University were involved in this study. AD was diagnosed according to the criteria of Hanifin and Rajka (6), and samples were collected from erythematous lesions on the face and neck. Routine skin care, including intermittent applications of mild steroid ointment or petrolatum, was administered before sampling. Written informed consent was obtained from each subject.

*Sequencing IGS 1 region from samples. Malassezia* samples were collected by applying transparent OpSite dressing (Smith and Nephew Medical, Ltd., Hull, U.K.), and fungal DNA was extracted from the OpSite dressing as described previously (16). The species-specific primer pair: Res-IGS-1F (5'-CGACCTAGTCGACTACATCCTAC) and Res-IGS-1R (5'-ATGAGGAGGAAAGGCAGGCAAG) were designed from the IGS 1 sequence analysis. The DNA pellet was resuspended in 30 μl of TE (10-mM Tris-HCl [pH 8.0], 1-mM EDTA [pH 8.0]). The DNA extracted (10 μl) from each sample was added to 40 μl of PCR master mixture, which consisted of 5 μl of 10× PCR buffer (TaKaRa), 4 μl of 200-μM deoxynucleoside triphosphates, 10 pmol of each primer, and 0.5 U of TaKaRa Ex *Taq* DNA polymerase (TaKaRa). PCR was performed with an initial denaturation at 94 C for 1 min, followed by 30 cycles of 30 sec at 94 C, 1 min at 54 C, and 30 sec at 72 C, and a final extension at 72 C for 10 min. The PCR products were cloned using a TA Cloning Kit (Invitrogen Corp., Calif., U.S.A.) and three positive clones were sequenced.

*Molecular phylogenetic analysis.* The sequences of the IGS 1 region obtained from the samples of AD patients and healthy subjects were aligned using Clustal W (20). For neighbor-joining analysis (13), the distances between sequences were calculated using Kimura's two-parameter model (8). A bootstrap analysis was conducted with 100 replications (5).

*Formation of chimeric molecules.* To confirm whether chimeric molecules formed under the PCR conditions used in this study, mixed genomic DNA from known *Malassezia* species (*M. dermatis, M. furfur, M. globosa, M. japonica, M. obtusa, M. slooffiae, M. sympodialis, M. pachydermatis*, and *M. yamatoensis*) was used for PCR co-amplification of the IGS region. Then, the IGS amplified from the mixed genomes was cloned; 30 clones were selected at random, and their sequences were determined.

## Results

*IGS 1 Sequence Analysis of* M. restricta

*Stock strains.* Complete sequences of the IGS 1 region were determined for three CBS stock strains of *M. restricta*. Their sizes ranged from 620 to 661 bp. *M. restricta* IGS 1 had two short sequence repeats (SSR) of (CA)n and (CT)n at positions 125–134 and 178–189 in the IGS sequence of strain CBS7877 (type strain), respectively. The nucleotide sequences determined in this study have been deposited with the DNA Data Bank of Japan (DDBJ) under accession numbers AB178809 (CBS7877), AB178808 (CBS7991), and AB178810 (CBS8747).

*Samples from subjects.* Before the IGS sequence analysis of the samples, formation of chimeric molecules was investigated. Thirty clones were chosen at random and sequenced; none were identified as a chimeric molecule. Using the PCR conditions described above, 454- to 515-bp fragments were partially amplified and analyzed. A phylogenetic tree was constructed from 28 IGS 1 sequences obtained from the samples of 13 AD patients, 12 healthy subjects, and three CBS stock strains (Fig. 1). The tree consisted of two major groups separated with 100% bootstrap support. Group 1 included 10 AD patients and three CBS stock strains, and Group 2 contained all 12 healthy subjects and three AD patients. The IGS 1 sequences derived from the AD patients (Group 1) were more diverse than those from the healthy subjects (Group 2). An alignment of the partial sequences of representative strains from Groups 1 and 2 is shown in Fig. 2. The sequence similarity between the two groups was below 70%. Two SSRs, (CA)n and (CT)n, were also found in the IGS 1 sequence from each sample. For both SSRs, there were more sequence repeats in the IGS 1 region of samples from the healthy subjects than from AD patients: (CA)n, AD patients, 6.8±3.9 repeats; healthy subjects, 14.7±1.2 repeats; (CT)n, AD patients, 6.8±2.0 repeats; healthy subjects, 9.7±1.9 repeats.

## Discussion

We have described differences in the IGS 1 genotypes of *M. restricta* colonizing the skin surfaces of AD patients and healthy subjects. rRNA gene sequences have been used for molecular phylogeny, taxonomy, and identification (10, 14). Of the subunits or regions in this gene, the IGS region shows remarkable intraspecies diversity. We have reported the analytical significance of the IGS region using *Cryptococcus neoformans* and *Trichosporon asahii* (15, 17). *M. globosa*, which is a

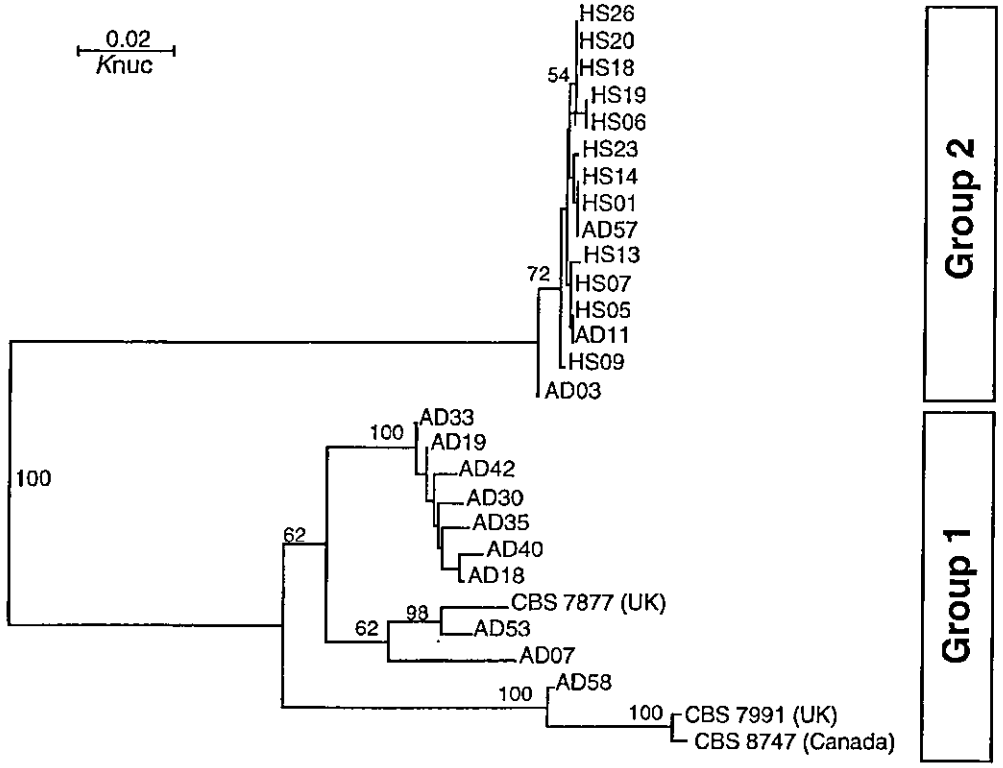


Fig. 1. Phylogenetic tree of *M. restricta* colonizing the skin surfaces of AD patients and healthy subjects based on DNA sequences of the IGS 1 region. AD, patient with atopic dermatitis; HS, healthy subject. The numbers are the confidence levels from 100 replicate bootstrap samplings (frequencies less than 50% are not shown). $K_{nuc}$, Kimura's parameter (8).

```
AD33          1 CGACCTAGTCGACTACATCCTACTGTATCCTACGCAATGGAGGTGTGTATGGTAGGTCAC
HS01          1 CGACCTAGTCGACTACATCCTACTGTATTCTACGCAATGGAGGTGTGTATTGTAGGACAC
                ***************************** ********************** ***** ***

AD33         61 ATCCTACCCCACTTTCCCATTCTTCTATACCTTACCCCCCTACCCCCTCTCTACGTCACC
HS01         61 AT-------------------------------------ACACCCACCCCACAT-A--
                **                                     ** *** * * ** * *

AD33        121 CGTGCACACACACA--------------------TTCACGCCTGTCTATGCGTCCCCCTC
HS01         79 ----CACACACACACACACACACACACACACAGTCGTCACCC----------------
                    **********                  **     *

AD33        161 CTCCAAGAGTCGAATTTCTCTCTCTCTCT----------CGTCAGTCTACTTGCCCATGG
HS01        119 -----------------CTCTCTCTCTCTCTCTCTCTCGTCAGTCTACTTGGCCATGT
                                 ************          ************** *****
```

Fig. 2. Alignment of the DNA sequences of the IGS 1 regions of representative sequences. AD, patient with atopic dermatitis; HS, healthy subject. The SSRs are underlined: (CA)n and (CT)n.

major cutaneous microflora, also has four genotypes (19). Of the four genotypes, two groups were found in AD patients; one group was from healthy subjects, and the other included samples from both AD patients and healthy subjects. This suggests that a specific genotype of *M. globosa* plays a significant role in AD. The present study also indicates that the IGS genotype of *M. restricta* obtained from AD patients is different from

that of healthy subjects. Three CBS stock strains were included in this study as reference strains; although they were isolated from healthy subjects, they are located in the AD cluster in the tree (Fig. 1). The CBS strains were from British or Canadian subjects. It is still not known whether our finding is specific for the Japanese population, or the CBS strains are an exception. This requires further analysis of *M. restricta* strains from other countries. The *M. restricta* IGS, like that of *M. globosa*, also has SSRs that could be used to distinguish microorganisms present in AD patients and healthy individuals.

The reason for the difference in the genotypes found in each population is unclear, but might reflect selection against *M. restricta* strains. There are three possible causes: (1) the effect of skin surface lipids, (2) the effect of ointments or cream bases, or (3) antifungal drug susceptibility. The main skin surface lipids are triglycerides, squalene, wax esters, cholesterol, ceramides, and free fatty acids (3). Although the lipid composition in AD patients is generally not different from that of healthy subjects, a significant decrease in ceramide 1 and differences in the concentrations of the related linoleate and oleate molecules have been reported (7, 24). Such differences in composition might affect colonization by *Malassezia* strains with different lipid requirements. The base ingredient of an ointment or cream can affect the growth of microorganisms, as with the growth of *M. furfur, M. globosa*, and *M. sympodialis* (9), but effects on *M. restricta* are unknown. Antifungal drug susceptibility might be responsible for selection of strains. A correlation between antifungal susceptibility and genotype has been reported in *Candida albicans* (23). However, because no patient in this study received antifungal therapy, this possibility can be excluded.

In conclusion, our IGS sequence analysis showed that the genotypes of *M. restricta* colonizing the skin surface of AD patients and healthy subjects are significantly different. Therefore, genotype should be considered when studying the relationship between *M. restricta* and AD.

This study was supported in part by Research Grant C (16590127) from the Japan Society for the Promotion of Science (TS).

## References

1) Ashbee, H.R., and Evans, E.G. 2002. Immunology of diseases associated with *Malassezia* species. Clin. Microbiol. Rev. **15**: 21–57.
2) Back, O., Scheynius, A., and Johansson, S.G. 1995. Ketoconazole in atopic dermatitis: therapeutic response is correlated with decrease in serum IgE. Arch. Dermatol. Res. **287**: 448–451.
3) Downing, D.T., Stewart, M.E., and Strauss, J.S. 1999. Lipids of the epidermis and the sebaceous glands, p. 144–155. *In* Freedberg, I.M., Eisen, A.Z., Wolff, K., Austen, K.F., Goldsmith, L.A., Katz, S.I., and Fitzpatrick, T.B. (eds), Fitzpatrick's dermatology in general medicine, 5th ed, McGraw-Hill, N.Y.
4) Faergemann, J. 2002. Atopic dermatitis and fungi. Clin. Microbiol. Rev. **15**: 545–563.
5) Felsenstein, J. 1985. Confidence limits on phylogenies: an approach using the bootstrap. Evolution **39**: 783–791.
6) Hanifin, J.M., and Rajka, G. 1980. Diagnostic features of atopic dermatitis. Acta Derm. Venereol. **92**: 4–47.
7) Hara, J., Higuchi, K., Okamoto, R., Kawashima, M., and Imokawa, G. 2000. High-expression of sphingomyelin deacylase is an important determinant of ceramide deficiency leading to barrier disruption in atopic dermatitis. J. Invest. Dermatol. **115**: 406–413.
8) Kimura, M. 1980. A simple method for estimation evolutionary rate of base substitutions through comparative studies of nucleotide sequences. J. Mol. Evol. **16**: 111–120.
9) Koyama, T., Kanbe, T., Kikuchi, A., and Tomita, Y. 2002. Effects of topical vehicles on growth of the lipophilic *Malassezia* species. J. Dermatol. Sci. **29**: 166–170.
10) Kurtzman, C.P., and Robnett, C.J. 1997. Identification of clinically important ascomycetous yeasts based on nucleotide divergence in the 5' end of the large-subunit (26S) ribosomal DNA gene. J. Clin. Microbiol. **35**: 1216–1223.
11) Leung, D.Y. 1995. Atopic dermatitis: the skin as a window into the pathogenesis of chronic allergic diseases. J. Allergy Clin. Immunol. **96**: 302–318.
12) Makimura, K., Murayama, Y.S., and Yamaguchi, H. 1994. Detection of a wide range of medically important fungal species by polymerase chain reaction (PCR). J. Med. Microbiol. **40**: 358–364.
13) Saitou, N., and Nei, M. 1987. The neighbor-joining method: a new method for reconstructing phylogenetic trees. Mol. Biol. Evol. **4**: 406–425.
14) Sugita, T., Nishikawa, A., Ikeda, R., and Shinoda, T. 1999. Identification of medically relevant *Trichosporon* species based on sequences of internal transcribed spacer regions and construction of a database for *Trichosporon* identification. J. Clin. Microbiol. **37**: 1985–1993.
15) Sugita, T., Ikeda, R., and Shinoda, T. 2001. Diversity among strains of *Cryptococcus neoformans* var. *gattii* as revealed by a sequence analysis of multiple genes and a chemotype analysis of capsular polysaccharide. Microbiol. Immunol. **45**: 757–768.
16) Sugita, T., Suto, H., Unno, T., Tsuboi, R., Ogawa, H., Shinoda, T., and Nishikawa, A. 2001. Molecular analysis of *Malassezia* microflora on the skin of atopic dermatitis patients and healthy subjects. J. Clin. Microbiol. **39**: 3486–3490.
17) Sugita, T., Nakajima, M., Ikeda, R., Matsushima, T., and Shinoda, T. 2002. Sequence analysis of the ribosomal DNA intergenic spacer 1 regions of *Trichosporon* species. J. Clin.

Microbiol. **40**: 1826–1830.
18) Sugita, T., Takashima, M., Kodama, M., Tsuboi, R., and Nishikawa, A. 2003. Description of a new yeast species, *Malassezia japonica*, and its detection in patients with atopic dermatitis and healthy subjects. J. Clin. Microbiol. **41**: 4695–4699.
19) Sugita, T., Kodama, M., Saito, M., Ito, T., Kato, Y., Tsuboi, R., and Nishikawa, A. 2003. Sequence diversity of the intergenic spacer region of the rRNA gene of *Malassezia globosa* colonizing the skin of patients with atopic dermatitis and healthy individuals. J. Clin. Microbiol. **41**: 3022–3027.
20) Thompson, J.D., Higgins, D.G., and Gibson, T.J. 1994. CLUSTAL W: improving the sensitivity of progressive multiple sequence alignment through sequence weighting, position-specific gap penalties and weight matrix choice. Nucleic Acids Res. **22**: 4673–4680.
21) Werfel, T., and Kapp, A. 1998. Environmental and other major provocation factors in atopic dermatitis. Allergy **53**: 731–739.
22) Wessels, M.W., Doekes, G., Van Ieperen-Van Kijk, A.G., Koers, W.J., and Young, E. 1991. IgE antibodies to *Pityrosporum ovale* in atopic dermatitis. Br. J. Dermatol. **125**: 227–232.
23) Xu, J., Ramos, A.R., Vilgalys, R., and Mitchell, T.G. 2000. Clonal and spontaneous origins of fluconazole resistance in *Candida albicans*. J. Clin. Microbiol. **38**: 1214–1220.
24) Yamamoto, A., Serizawa, S., Ito, M., and Sato, Y. 1991. Stratum corneum lipid abnormalities in atopic dermatitis. Arch. Dermatol. Res. **283**: 219–223.

Microbiol. Immunol., 48(8), 579–583, 2004

# A New Yeast, *Malassezia yamatoensis*, Isolated from a Patient with Seborrheic Dermatitis, and Its Distribution in Patients and Healthy Subjects

**Takashi Sugita*[,1], Mami Tajima[2], Masako Takashima[3], Misato Amaya[2], Masuyoshi Saito[2], Ryoji Tsuboi[2], and Akemi Nishikawa[4]**

[1]*Department of Microbiology and* [4]*Department of Immunobiology, Meiji Pharmaceutical University, Kiyose, Tokyo 204–8588, Japan,* [2]*Department of Dermatology, Tokyo Medical University, Shinjuku-ku, Tokyo 160–0023, Japan, and* [3]*Japan Collection of Microorganisms, RIKEN (The Institute of Physical and Chemical Research), Wako, Saitama 351–0198, Japan*

Received March 22, 2004; in revised form, May 7, 2004. Accepted May 14, 2004

*Abstract*: **Over the last few years, new *Malassezia* species have been found regularly in Japanese subjects. We isolated another new *Malassezia* species from a Japanese patient with seborrheic dermatitis (SD), and named it *M. yamatoensis*. In its physiological characteristics and the utilization of Tween by *M. yamatoensis* is similar to that of *M. furfur* and *M. dermatis*. It is distinguished by its growth temperature. To examine the distribution of the microorganism in the skin of patients with SD and atopic dermatitis (AD), and healthy subjects, we applied transparent dressings to the skin, and detected *M. yamatoensis* DNA using a non-culture-based method that consisted of nested PCR with specific primers. *M. yamatoensis* DNA was detected from 3 of 31 SD patients (9.7%), 5 of 36 AD patients (13.9%), and 1 of 22 healthy subjects (4.6%). Therefore, *M. yamatoensis* is a rare member of the cutaneous microflora.**

*Key words*: ***Malassezia yamatoensis*, New species, Seborrheic dermatitis, Microflora**

With the exception of *Malassezia pachydermatis*, *Malassezia* species require a lipid for growth, and are part of the human cutaneous microflora. In dermatology, *Malassezia* species are important fungi clinically, as they are associated with pityriasis versicolor, seborrheic dermatitis (SD), *Malassezia* folliculitis, and atopic dermatitis (AD) (2–4). Although *M. furfur* was previously thought to be the causative agent or trigger factor in all of these skin diseases, Guého et al. (6) reclassified this microorganism into several species in 1996. Based on the new taxonomy of the genus *Malassezia*, several studies have examined the relationship between the newly defined species and skin diseases (1, 7, 8, 12). Our research group has also analyzed the cutaneous microflora of AD patients and healthy subjects using a molecular-based non-culture method (17, 19). During these studies, we isolated two new *Malassezia* species from Japanese AD patients and healthy subjects: *M. dermatis* (18) and *M. japonica* (20). Subsequently, we analyzed the cutaneous microflora of SD patients and found an additional new *Malassezia* species. In this paper, we propose a new species, *M. yamatoensis*, and describe the distribution of this microorganism in the skin of SD and AD patients, and healthy subjects.

**Address correspondence to* Dr. Takashi Sugita, Department of Microbiology, Meiji Pharmaceutical University, 2-522-1 Noshio, Kiyose, Tokyo 204–8588, Japan. Fax: +81–424–95–8762. E-mail: sugita@my-pharm.ac.jp

## Materials and Methods

*Strains.* Two *Malassezia* strains (M 9985 and M 9986) were isolated from a lesion on the wing of the nose of a 30-year-old male SD patient. OpSite transparent dressings (Smith and Nephew Medical, Ltd., Hull, U.K.) were applied to the skin of the SD patient and then transferred onto modified Leeming and Notman agar (10 g glucose, 10 g peptone, 8 g bile salts (OXOID, Hampshire, U.K.), 2 g yeast extract, 0.5 g glycerol monostearate, 15 g agar, 10 ml glycerol, 5 ml Tween 60, 20 ml olive oil, and 50 mg chloramphenicol (Sankyo, Tokyo) per liter) as recommended by the Centraalbureau voor Schimmelcultures, and incubated at 32 C.

*rDNA sequencing and phylogenetic analysis.* In the rRNA gene, D1/D2 26S rDNA, the internal transcribed spacer (ITS) region including 5.8S rDNA, and inter-

*Abbreviations*: AD, atopic dermatitis; SD, seborrheic dermatitis.

genic spacer (IGS) 1 region were sequenced directly from PCR products using the primer pairs NL-1 (5'-GCATATCAATAAGCGGAGGAAAAG) and NL-4 (5'-GGTCCGTGTTTCAAGACGG) (11), pITS-F (5'-GTCGTAACAAGGTTAACCTGCGG) and pITS-R (5'-TCCTCCGCTTATTGATATGC) (16), and 26SBF (5'-AGCTGCTGCCAATGCTAGCTC) and Mala-R (5'-TACTGCTGTGAATGCTCCAGC) (20), respectively. The PCR products were sequenced using an ABI 310 DNA sequencer and a BigDye Terminator Cycle Sequencing Ready Reaction kit (Perkin-Elmer Applied Biosystems, Calif., U.S.A.) according to the manufacturer's instructions. The sequences were aligned using Clustal W software (21). For a neighbor-joining analysis (15), the distances between sequences were calculated using Kimura's two-parameter model (10). A bootstrap analysis was conducted with 100 replications (5).

*Taxonomic characteristics.* Tween 20, 40, 60, and 80 utilization, catalase reactions, and diazonium blue B (DBB) reactions were performed, as described by Guého et al. (6). The morphology was examined on modified Leeming and Notman agar (LNA) after incubation at 32 C for 7 days. Ubiquinone molecules were identified using the method of Nakase and Suzuki (13).

*Direct DNA detection in samples from patients with atopic dermatitis, seborrheic dermatitis, and healthy subjects.*

*i) Subjects.* To examine the distribution of *M. yamatoensis* on the skin of patients and healthy subjects, 31 SD outpatients (25 males, 6 females; aged from 20 to 79, mean 48.2±18.6 years) and 36 AD outpatients (24 males, 12 females; aged from 20 to 64, mean 33.3±10.5 years) at Tokyo Medical University Hospital and 22 healthy students (7 males, 15 females; aged from 19 to 25, mean 20.7±1.6 years old) at Meiji Pharmaceutical University were involved in this study. Written informed consent was obtained from each subject.

*ii) Design of* M. yamatoensis *species-specific primers for PCR.* From the sequence of the IGS1 region, *M. yamatoensis*-specific primers were designed: Yama-IGS1F (5'-CGATCAAACTTCTCTGTGTCCAG) and Yama-IGS1R (5'-TGTGTGGGAGGTAGAAGAGGCA). The primers' specificity was confirmed using the strains of *M. yamatoensis* and known *Malassezia* species (*M. dermatis, M. furfur, M. globosa, M. japonica, M. obtusa, M. pachydermatis, M. restricta, M. slooffiae*, and *M. sympodialis*) as shown in Table 1.

Table 1. Specificity of the primers for *Malassezia yamatoensis* and related species

| Species | Strain | Specificity | |
|---|---|---|---|
| | | 26SBF and Mala-R | Yama-IGS1F and Yama-IGS1R |
| *Malassezia yamatoensis* sp. nov. | M 9985 | + | + |
| | M 9986 | + | + |
| *Malassezia dermatis* | M 9927 | − | − |
| | M 9929 | − | − |
| *Malassezia furfur* | CBS 4162 | + | − |
| | CBS 6000 | + | − |
| | CBS 7982 | + | − |
| *Malassezia globosa* | CBS 7966 | + | − |
| | M 9972 | + | − |
| *Malassezia japonica* | M 9966 | + | − |
| | M 9967 | + | − |
| *Malassezia obtusa* | CBS 7876 | + | − |
| | Clinical isolate 2-17 | + | − |
| *Malassezia pachydermatis* | CBS 1879 | + | − |
| *Malassezia restricta* | CBS 7991 | + | − |
| | M 9976 | + | − |
| *Malassezia slooffiae* | CBS 7956 | + | − |
| | M 9980 | + | − |
| *Malassezia sympodialis* | CBS 7222 | − | − |
| | M 9978 | − | − |
| *Candida albicans* | CBS 562 | − | − |
| *Candida guilliermondii* | CBS 566 | − | − |
| *Candida parapsilosis* | CBS 604 | − | − |
| *Rhodotorula mucilaginosa* | CBS 17 | − | − |

CBS, Centraal Bureau voor Schimmelcultures, Baarn, The Netherlands; M, Meiji Pharmaceutical University, Tokyo, Japan.

+, positive reaction; −, negative reaction.

*iii) Analysis of the* M. yamatoensis *microflora. Malassezia* DNA was extracted from the OpSite dressings using a previously described method (17). The DNA (3 μl) extracted from each sample was added to 47 μl of the PCR master mixture. PCR was performed with an initial denaturation at 94 C for 3 min, followed by 30 cycles of 30 sec at 94 C, 1 min at 57 C, and 30 sec at 72 C, and a final extension at 72 C for 10 min with primers 28SBF and Mala-R. In the nested PCR step, 1 μl of the first amplification product was added to a new reaction mixture. The PCR consisted of an initial denaturation at 94 C for 3 min, followed by 30 cycles of 30 sec at 94 C, 1 min at 59 C, and 15 sec at 72 C, and a final extension at 72 C for 10 min with primers Yama-IGS1F and Yama-IGS1R. We confirmed the absence of false positive reactions by determining the DNA sequences of the PCR products after cloning them in pCR2.1 vector (Invitrogen), since various species, including bacteria and filamentous fungi, colonize the skin surface.

## Results and Discussion

*M. yamatoensis* clustered with *M. furfur, M. obtusa,* and *M. japonica* with 93% bootstrap support on trees constructed using the D1/D2 26S rDNA (Fig. 1). The dissimilarity between the D1/D2 26S rRNA gene of the isolates and these three phylogenetically close species exceeded 4.6%. The DNA sequence of the ITS region of *M. yamatoensis* differs by approximately 40%. The divergence between *M. yamatoensis* and known *Malassezia* species is sufficient to resolve them as individual species (14, 16). The nucleotide sequences (D1/D2 26S rDNA, ITS, and IGS regions) determined in this study have been deposited with the DNA Data Bank of Japan (DDBJ), as AB125261 to AB125266. The physiological characteristics of *M. yamatoensis* and other *Malassezia* species are shown in Table 2. The characteristics of *M. yamatoensis* are similar to those of *M. dermatis* and *M. furfur*, but *M. yamatoensis* cannot

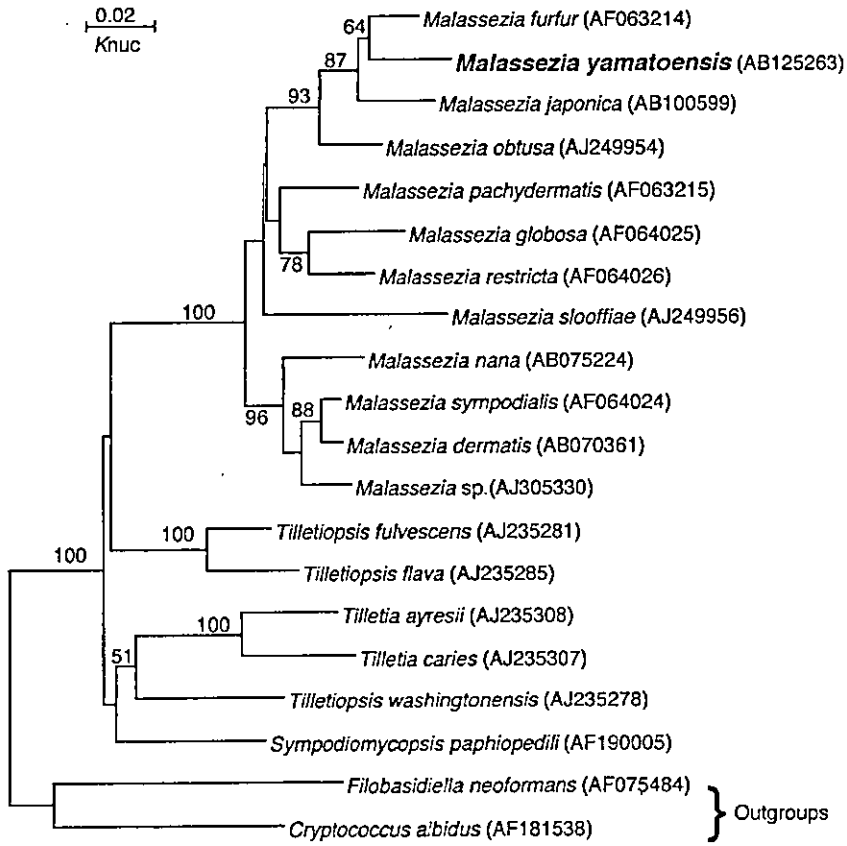


Fig. 1. Phylogenetic trees constructed using the D1/D2 26S rDNA sequences of *M. yamatoensis* and related Ustilaginomycetes species. The DDBJ/GenBank accession numbers are indicated in parentheses. The numerals are the confidence level from 100 replicate bootstrap samplings (frequencies less than 50% are not indicated). *K*nuc, Kimura's parameter (10).

Table 2. Physiological characteristics of *Malassezia yamatoensis* and other *Malassezia* species

| Species | Growth on SDA[a] at 32 C | Growth on mDixon[f] at | | | Catalase reaction | Utilization of | | | |
|---|---|---|---|---|---|---|---|---|---|
| | | 32 C | 37 C | 40 C | | 10% Tween 20 | 0.5% Tween 40 | 0.5% Tween 60 | 0.1% Tween 80 |
| *Malassezia yamatoensis* | − | + | + | − | + | + | + | + | + |
| *Malassezia dermatis*[a] | − | + | + | + | + | + | + | + | + |
| *Malassezia sympodialis*[b] | − | + | + | + | + | − | + | + | + |
| *Malassezia furfur*[b] | − | + | + | + | + | + | + | + | + |
| *Malassezia nana*[c] | − | + | + | +/− | + | +/− | + | + | ± |
| *Malassezia slooffiae*[b] | − | + | + | + | + | ± or + | + | + | − |
| *Malassezia japonica*[d] | − | + | + | − | + | − | ± | + | − |
| *Malassezia globosa*[b] | − | + | ± or − | − | + | − | − | − | − |
| *Malassezia obtusa*[b] | − | + | ± or + | − | + | − | − | − | − |
| *Malassezia restricta*[b] | − | + | + | − | − | − | − | − | − |
| *Malassezia pachydermatis*[b] | + | + | + | + | ± or + | − | + | + | + |

[a] Sugita et al. (18).
[b] Guého et al. (6).
[c] Hirai et al. (9).
[d] Sugita et al. (20).
[e] Sabouraud dextrose agar.
[f] modified Dixon agar.
+, positive; −, negative; ±, weakly positive.

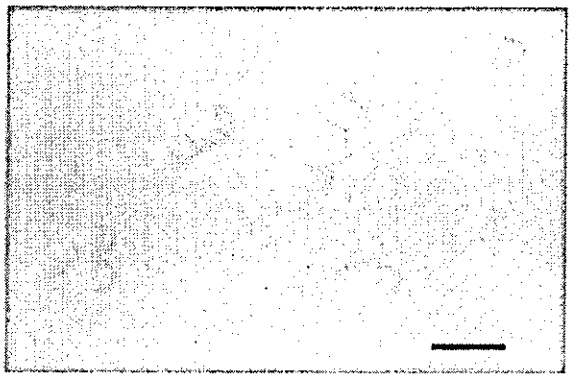

Fig. 2. Vegetative cells of *Malassezia yamatoensis* M 9985 grown in LNA for 7 days at 32 C. The scale bar indicates 10 μm.

grow at 40 C.

We analyzed 268 samples from 89 subjects (62 samples from 31 SD patients, 140 samples from 36 AD patients, 66 samples from 22 healthy subjects). *M. yamatoensis* was detected in only 3 SD patients (9.7%), 5 AD patients (13.9%), and 1 healthy subject (4.6%). As *M. yamatoensis* is a minor member of the microflora in human skin, this microorganism is thought not to be a major participant in skin disease. Since Guého et al. (6) proposed a new taxonomy of the genus *Malassezia* in 1996, four new *Malassezia* species have been found. Of these four species, *M. nana* (9) was isolated from animals, and our research group found three (*M. dermatis* (18), *M. japonica* (20), and *M. yamatoensis* (this study)) on humans.

In conclusion, *M. yamatoensis* is a new member of the cutaneous microflora on humans, although it is not a major member of the microflora. Its taxonomic description is also stated.

*Latin Diagnosis of* Malassezia yamatoensis *Sugita, Takashima, Tajima, Tsuboi et Nishikawa sp. nov.*

In LNA, post dies 6 ad 32 C, cellulae vegetativae, ovoideae vel ellipsoideae (2–4.5)×(2–7.5) μm, e basi lata gemmantes. Cultura xanthoalba, semi-nitida, rugosa, interdum plicata, et butyracea et margo glabra aut lobulata. In agaro glucoso-peptonico Tween 20 (10%), 40 (0.5%), 60 (0.5%) et 80 (0.1%) addito crescit. 37 C crescit neque 40 C. H2O2 hydrolysatur. Commutatio colori per diazonium caeruleum B positiva. Ubiquinonum majus Q-9 est. Teleomorphis ignota. Typus M 9985$^T$ isolatus ex cute seborrhea humani, Tokyo, Japonia, vii, 2003, M. Tajima et T. Sugita, conservatur in collectionibus culturarum in 'Japan Collection of Microorganisms,' Saitama, Japonia ut JCM 12262$^T$, item in 'Centraalbureau voor Schimmelcultures (CBS),' Utrecht, Hollandia ut CBS 9725$^T$ sustentat.

*Description of* Malassezia yamatoensis *Sugita, Takashima, Tajima, Tsuboi et Nishikawa sp. nov.*

On LNA, after 6 days at 32 C, the vegetative cells are oval to ellipsoidal (2–4.5)×(2–7.5) μm with buds formed on the narrow base. The colony is yellowish white, semi-shining, wrinkled or sometimes folded, and butyrous, and has an entire lobed margin. Growth occurs on glucose/peptone agar supplemented with Tween 20 (10%), 40 (0.5%), 60 (0.5%) and 80 (0.1%) as sole source of lipid. Good growth occurs at 37 C but

not 40 C. Catalase reaction is positive. The diazonium blue B reaction was positive. The major ubiquinone is Q-9. Teleomorph is unknown.

The type strain M 9985$^T$, isolated from skin of a Japanese patient with seborrheic dermatitis in Tokyo, Japan, by M. Tajima and T. Sugita in July, 2003, is maintained in the Japan Collection of Microorganisms (JCM), Saitama, Japan as JCM 12262$^T$, and the Centraalbureau voor Schimmelcultures (CBS), Utrecht, The Netherlands as CBS 9725$^T$. The other strain, M 9986 has also been deposited in the JCM and CBS, as JCM 12263 and CBS 9726, respectively.

Etymology. From Yamato, the old name of Japan where the type strain of this species was obtained.

This study was supported in part by a Grant-in-Aid for the Promotion of the Advancement of Education and Research in Graduate Schools from the Ministry of Education, Culture, Sports, Science and Technology, Japan, and a Grant-in-Aid for Scientific Research (B) from the Japan Society for the Promotion of Science.

## References

1) Aspiroz, C., Ara, M., Varea, M., Rezusta, A., and Rubio, C. 2002. Isolation of *Malassezia globosa* and *M. sympodialis* from patients with pityriasis versicolor in Spain. Mycopathologia **154**: 111–117.
2) Ashbee, H.R., and Evans, E.G. 2002. Immunology of diseases associated with *Malassezia* species. Clin. Microbiol. Rev. **15**: 21–57.
3) Faergemann, J. 1998. The role of *Malassezia* species in the ecology of human skin and as pathogens. Med. Mycol. **36** (Suppl 1): 220–229.
4) Faergemann, J. 2002. Atopic dermatitis and fungi. Clin. Microbiol. Rev. **15**: 545–563.
5) Felsenstein, J. 1985. Confidence limits on phylogenies: an approach using the bootstrap. Evolution **39**: 783–791.
6) Guého, E., Midgley, G., and Guillot, J. 1996. The genus *Malassezia* with description of four new species. Antonie Leeuwenhoek **69**: 337–355.
7) Gupta, A.K., Kohli, Y., Faergemann, J., and Summerbell, R.C. 2001. Epidemiology of *Malassezia* yeasts associated with pityriasis versicolor in Ontario, Canada. Med. Mycol. **39**: 199–206.
8) Gupta, A.K., Kohli, Y., Summerbell, R.C., and Faergemann, J. 2001. Quantitative culture of *Malassezia* species from different body sites of individuals with or without dermatoses. Med. Mycol. **39**: 243–251.
9) Hirai, A., Kano, R., Makimura, K., Duarte, E.R., Hamdan, J.S., Lachance, M.A., Yamaguchi, H., and Hasegawa, A. 2003. *Malassezia nana* sp. nov., a novel lipid-dependent yeast species isolated from animals. Int. J. Syst. Evol. Microbiol. in press.
10) Kimura, M. 1980. A simple method for estimating evolutionary rate of base substitutions through comparative studies of nucleotide sequences. J. Mol. Evol. **16**: 111–120.
11) Kurtzman, C.P., and Robnett, C.J. 1997. Identification of clinically important ascomycetous yeasts based on nucleotide divergence in the 5′ end of the large-subunit (26S) ribosomal DNA gene. J. Clin. Microbiol. **35**: 1216–1223.
12) Nakabayashi, A., Sei, Y., and Guillot, J. 2000. Identification of *Malassezia* species isolated from patients with seborrhoeic dermatitis, atopic dermatitis, pityriasis versicolor and normal subjects. Med. Mycol. **38**: 337–341.
13) Nakase, T., and Suzuki, M. 1986. *Bullera megalospora*, a new species of yeast forming large ballistospores isolated from dead leaves of *Oryza sativa, Miscanthus sinensis*, and *Sasa* sp. in Japan. J. Gen. Appl. Microbiol. **32**: 225–240.
14) Peterson, S.W., and Kurtzman, C.P. 1991. Ribosomal RNA sequence divergence among sibling species of yeasts. System. Appl. Microbiol. **14**: 124–129.
15) Saitou, N., and Nei, M. 1987. The neighbor-joining method: a new method for reconstructing phylogenetic trees. Mol. Biol. Evol. **4**: 406–425.
16) Sugita, T., Nishikawa, A., Ikeda, R., and Shinoda, T. 1999. Identification of medically relevant *Trichosporon* species based on sequences of internal transcribed spacer regions and construction of a database for *Trichosporon* identification. J. Clin. Microbiol. **37**: 1985–1993.
17) Sugita, T., Suto, H., Unno, T., Tsuboi, R., Ogawa, H., Shinoda, T., and Nishikawa, A. 2001. Molecular analysis of *Malassezia* microflora on the skin of atopic dermatitis patients and healthy subjects. J. Clin. Microbiol. **39**: 3486–3490.
18) Sugita, T., Takashima, M., Shinoda, T., Suto, H., Unn, T., Tsuboi, R., Ogawa, H., and Nishikawa, A. 2002. New yeast species, *Malassezia dermatis*, isolated from patients with atopic dermatitis. J. Clin. Microbiol. **40**: 1363–1367.
19) Sugita, T., Kodama, M., Saito, M., Ito, M., Kato, Y., Tsuboi, R., and Nishikawa, A. 2003. Sequence diversity of the intergenic spacer region of the rRNA gene of *Malassezia globosa* colonizing the skin of patients with atopic dermatitis and healthy individuals. J. Clin. Microbiol. **41**: 3022–3027.
20) Sugita, T., Takashima, M., Kodama, M., Tsuboi, R., and Nishikawa, A. 2003. Description of a new yeast species, *Malassezia japonica*, and its detection in patients with atopic dermatitis and healthy subjects. J. Clin. Microbiol. **41**: 4695–4699.
21) Thompson, J.D., Higgins, D.G., and Gibson, T.J. 1994. CLUSTAL W: improving the sensitivity of progressive multiple sequence alignment through sequence weighting, position-specific gap penalties and weight matrix choice. Nucleic Acids Res. **22**: 4673–4680.

Original Paper

nephron
Experimental
Nephrology

Nephron Exp Nephrol 2004;98:e100–e108
DOI: 10.1159/000080685

Received: November 25, 2003
Accepted: June 11, 2004

# Activation of the Smad Pathway in Glomeruli from a Spontaneously Diabetic Rat Model, OLETF Rats

Yoko Furuse[a] Naotake Hashimoto[c] Mamiko Maekawa[b] Yoshiro Toyama[b]
Atsuhito Nakao[d] Itsuo Iwamoto[a] Kenichi Sakurai[a] Yoshifumi Suzuki[e]
Kazuo Yagui[a] Shigeki Yuasa[f] Kiyotaka Toshimori[b] Yasushi Saito[a]

Departments of [a]Clinical Cell Biology and [b]Anatomy and Developmental Biology, Graduate School of Medicine, Chiba University, Chiba; [c]Department of Diabetes and Metabolic Disease, Asahi General Hospital, Asahi, Chiba; [d]Department of Immunology, University of Yamanashi Faculty of Medicine, Yamanashi; [e]Department of Internal Medicine, Matsudo General Hospital, Matsudo, Chiba, and [f]Department of Ultrastructural Research, National Institute of Neuroscience, National Center of Neurology and Psychiatry, Tokyo, Japan

**Key Words**
Smads · Transforming growth factor-β · OLETF · Diabetic nephropathy · Glomerulus

**Abstract**
***Background/Aims:*** Transforming growth factor-β (TGF-β) mediates the excess accumulation of extracellular matrix in the diabetic kidney. Smad family proteins have been identified as signal transducers for the TGF-β superfamily. We sought to characterize the role of Smad proteins in mediating TGF-β responses in the development of diabetic nephropathy. ***Methods:*** We evaluated the time course of TGF-$\beta_1$ fibronectin, Smad2 and Smad3 protein expression and Smad3 activation in glomeruli from spontaneously diabetic Otsuka Long-Evans Tokushima Fatty (OLETF) rats, using immunohistochemistry and Western blot analysis. ***Results:*** The glomeruli of diabetic OLETF rats showed not only accelerated activation of Smad3, but also enhanced protein expression of Smad2 and Smad3, which occurred in parallel to the increased expression of TGF-β and fibronectin compared with glomeruli of control, Long-Evans Tokushima Otsuka (LETO) rats at 30 weeks of age. No differences were found in TGF-$\beta_1$ fibronectin, Smad2 and Smad3 protein expression and Smad3 activation in glomeruli between the two strains at 12 weeks of age when OLETF rats were not diabetic. ***Conclusions:*** The enhancement of Smad protein expression and activation may be involved in the TGF-β signaling cascade that plays an important role in the development of diabetic nephropathy through progressive expansion of the mesangial matrix.



## Introduction

Diabetic glomerulopathy is characterized by progressive expansion of the mesangial matrix without evidence of increased mesangial cell proliferation [1, 2]. Many studies have implicated the involvement of transforming growth factor-β (TGF-β) in various human renal diseases

KARGER
Fax + 41 61 306 12 34
E-Mail karger@karger.ch
www.karger.com


1660–2129/04/0983–0100$21.00/0

Accessible online at:
www.karger.com/nce

Naotake Hashimoto, MD
Department of Diabetes and Metabolic Disease, Asahi General Hospital
1-1326, Asahi, Chiba 289-2511 (Japan)
Tel. +81 479 638111, Fax +81 479 638580
E-Mail naohasi@hospital.asahi.chiba.jp

that are characterized by the accumulation of extracellular matrix including diabetic nephropathy [3–6]. In vitro, high glucose concentrations increase TGF-β expression and matrix synthesis in renal cells [7–9]. It has been demonstrated that a neutralizing antibody against TGF-β and a TGF-β antisense oligonucleotide can reduce the high glucose-induced increase in collagen or fibronectin production by mesangial cells [10, 11]. Paracrine-produced TGF-β induces accumulation of the glomerular extracellular matrix in the renal tissue of transgenic mice [12]. These lines of evidence prove that autocrine and paracrine effects of activated TGF-β play a crucial role in the progression of diabetic nephropathy.

The Smad protein family has been identified as an essential component of the intracellular signaling system for TGF-β. Smad2 and Smad3 show a high degree of structural homology and mediate signaling by TGF-β. The receptor complex activated by TGF-β binding phosphorylates Smad2 or Smad3 [13–16]. Smad4 forms a heteromeric complex with phosphorylated Smad2 or Smad3, and then the complex translocates to the nucleus and regulates transcriptional responses [17]. TGF-β-mediated phosphorylation of Smad2 or Smad3 is inhibited by Smad7, suggesting that its antagonistic effect is exerted at an important regulatory step [18]. Therefore, elucidation of the role of the Smad family proteins in diabetic kidneys may be important for clarifying the pathogenesis and treatment of diabetic nephropathy.

The Otsuka Long-Evans Tokushima Fatty (OLETF) rat exhibits obesity, late onset of hyperglycemia (after 18 weeks of age), hyperinsulinemia, and proteinuria. This rat has been utilized extensively as a model of type 2 diabetes mellitus [19–21]. The OLETF rat develops histological abnormalities specific to human diabetic nephropathy such as mesangial expansion and thickening of the glomerular basement membrane [20, 22].

In the present study, we examined protein expression and activation of the Smad-mediated pathway and its role as a downstream effector of TGF-β signaling in the progression of diabetic nephropathy using OLETF rats.

## Materials and Methods

*Animals*

Male OLETF rats were utilized at the age of 12 and 30–39 weeks and age-matched male Long-Evans Tokushima Otsuka (LETO) rats served as controls. Both strains were obtained from the Tokushima Research Institute of Otsuka Pharmaceutical Co. (Tokushima, Japan). All rats were allowed free access to food and water. When rats were anesthetized, their body weight was measured and blood was obtained from the aorta. Blood glucose levels were measured by an electrode meter (Glucocard; Kyoto Daiichi, Kyoto, Japan). Serum immunoreactive insulin (IRI) was determined by a rat insulin radioimmunoassay kit (St. Charles, Mo., USA) according to the manufacturer's instructions. Urinary albumin was measured by an enzyme-linked immunosorbent assay kit (Exocell Inc., Philadelphia, Pa., USA) according to the manufacturer's instructions. Experiments were performed in compliance with the Principles of Laboratory Animal Care (NIH publ. No. 85-23, revised 1985).

*Antibodies*

Antibodies were purchased from the following vendors: rabbit polyclonal anti-TGF-$\beta_1$ antibody and fluorescein-conjugated antibody to rabbit IgG from Santa Cruz Biotechnology (Santa Cruz, Calif., USA); mouse monoclonal anti-Smad2 antibody from Transduction Laboratories (Lexington, Ky., USA); rabbit polyclonal anti-fibronectin antibody from Chemicon International (Temecula, Calif., USA); rabbit polyclonal anti-Smad3 antibody from Zymed Laboratories (South San Francisco, Calif., USA); fluorescein-conjugated antibody to mouse IgG from Kirkegaard & Perry Laboratories (Gaithersburg, Md., USA); horseradish peroxidase-conjugated antibody to rabbit IgG from Calbiochem (Darmstadt, Germany); horseradish peroxidase-conjugated antibody to mouse IgG from ICN Biomedicals (Irvine, Calif., USA); biotin-conjugated antibody to rabbit IgG from Vector Laboratories (Burlingame, Calif., USA).

*Renal Tissue Specimens*

Rats were anesthetized and fixed by transcardiac perfusion with a solution of 4% paraformaldehyde and 0.5% picric acid in phosphate-buffered saline (PBS). Kidneys were removed and immersed in the same fixative for 2 h at 4°C. Pieces of the cortex of kidneys were embedded in OCT compound (Sakura Finetechnical Co., Ltd, Tokyo, Japan) for producing cryostat sections. Some pieces of the cortices were paraffin-embedded.

*Light Microscopy*

Sections (5 μm thick) of the paraffin-embedded tissue were cut and deparaffinized by treatment with xylene, followed by graded ethanol. All sections were stained with periodic acid-Schiff (PAS) and counterstained with Mayer's hematoxylin to examine renal pathological changes. The specimens were examined under the light microscope.

*Immunofluorescence Staining*

Sections (20 μm thick) from the kidney tissue embedded in OCT compound were prepared using on a cryostat. Indirect immunofluorescence staining was carried out using fluorescein-conjugated secondary antibodies for evaluation of protein expression of TGF-$\beta_1$, fibronectin and Smad2 in glomeruli. All sections were washed in PBS to remove the OCT compound and incubated in PBS containing 10% Normal Goat Serum (NGS) (Gibco) and 0.1% Triton X-100 (Sigma Chemical Co., St. Louis, Mo., Japan) for 1 h at room temperature to block non-specific protein-binding sites. Subsequently, they were incubated with the primary antibodies (anti-TGF-$\beta_1$ antibody, at 1:50 dilution; anti-Smad2 antibody, at 1:30 dilution; or anti-fibronectin antibody, at 1:250 dilution) overnight at 4°C. After three 5-min washes in PBS, the sections were incubated with fluorescein-conjugated secondary antibody appropriate for the species of primary antibody used for 1 h at room temperature. The sections were washed with three 5-min washes in PBS and then mounted with

PermaFluor Aqueous Mounting Medium (Shandon, Pittsburgh, Pa., USA). The specimens were observed using a confocal laser scanning microscope (MRC-600, BioRad). Negative controls were performed without primary antibodies.

Glomeruli were randomly selected for a quantitative analysis in each section immunostained for TGF-$\beta_1$, fibronectin and Smad2 by the immunofluorescence method and sections of negative controls. The criterion for selection was a cross-sectional cut through or near the vascular poles. Seven to sixteen glomeruli were examined from at least 3 rats from each group. The average value of fluorescence intensity in each glomerulus was calculated by using NIH image 1.61 software (shareware from NIH, Bethesda, Md., USA). TGF-G$\beta_1$, fibronectin and Smad2 protein expression in the glomeruli was evaluated by the score yielded after subtracting the value for the negative controls from the value for sections immunostained for each protein.

*Immunoperoxidase Staining*

Immunolocalization of Smad3 was studied using an avidin-biotin complex peroxidase kit. Sections (5 μm thick) of paraffin-embedded tissue were cut. Following deparaffinization, endogenous peroxidase activity was quenched by incubating the tissue with 0.3% hydrogen peroxide in methanol for 30 min. Non-specific protein-binding sites were blocked with PBS containing 1% bovine serum albumin and 5% NGS for 30 min at room temperature. The sections were incubated overnight at 4°C with rabbit polyclonal anti-Smad3 antibody at 1:100 dilution. The same concentration of rabbit IgG was used as a negative control. After three 5-min washes with PBS, they were incubated with biotin-conjugated antibody to rabbit IgG in PBS with 1.5% NGS for 30 min at room temperature. Subsequently, the sections were incubated with ABC reagent: Vectastain Elite avidin-biotin complex peroxidase kit from Vector Laboratories according to the manufacturer's instructions. The bound peroxidase was detected by a 5-min reaction with hydrogen peroxide and 3,3′-diaminobenzidine tetrahydrochloride (Sigma Chemical Co.) as substrates. Mayer's hematoxylin was used as the counterstain.

Glomeruli were randomly selected for a quantitative analysis in each section immunostained for Smad3. Twenty to fifty glomeruli were examined from at least 3 rats from each group. We counted the number of immunostained nuclei in a glomerulus and calculated the ratio to the total number of the glomerular component cells. The number of component cells in each glomerulus was obtained by counting the hematoxylin-stained nuclei.

*Western Blot Analysis*

Rats were anesthetized and perfused in situ via the aorta with PBS (pH 7.4) to remove blood. The kidneys were excised, and the cortices were then cut into pieces. A plastic rod was used to pass the minced cortex through a 600-μm stainless mesh. The tissue that emerged through the mesh was then passed sequentially through 150-, 130-, 110-, and 90-μm filters. Intact glomeruli retained on the 110- or 90-μm filters were resuspended in ice-cold PBS, collected by centrifugation at 1,500 rpm for 5 min at 4°C. Specimens were >95% free of extraglomerular elements. Isolated glomeruli were homogenized in cell lysis buffer (100 m*M* sodium fluoride, 10 m*M* sodium pyrophosphate, 5 m*M* EDTA pH 8.0, 150 m*M* NaCl, 1% Triton X-100, 10 μg/ml bacitracin, 10 μg/ml pepstatin, 10 μg/ml leupeptin, 10 μg/ml chymostatin, 10 μg/ml aprotinin, 10 μg/ml antipain, and 0.3 mg/ml PMSF dissolved in 50 m*M* Hepes pH 7.6). The tissue homogenates were centrifuged at 15,000 rpm for 15 min at 4°C to pellet insoluble material. The protein concentrations of the supernatants were determined by BCA Protein Assay Reagent A (Pierce, Rockford, Ill., USA). Western blot analysis was performed according to the method reported previously [23] with some modifications. Protein samples (12 μg) were fractionated by electrophoresis in a polyacrylamide gel and transferred to a nitrocellulose membrane. The blot was probed with the primary antibody (rabbit polyclonal anti-TGF-$\beta_1$ antibody, 0.2 μg/ml, mouse monoclonal anti-Smad2 antibody, 0.5 μg/ml or rabbit polyclonal anti-Smad3 antibody, 2.5 μg/ml) and incubated with horseradish peroxidase-conjugated secondary antibody appropriate for the species of primary antibody used, and then visualized by chemiluminescence using a ECL kit (Amersham Biosciences, Bucks., UK). Western blot analysis was performed on 2–4 samples from different animals.

*Statistical Analysis*

All values are expressed as the mean ± SE. Statistical analysis was carried out using the Mann-Whitney U test. Differences were considered statistically significant at $p < 0.05$.

## Results

*Metabolic Data*

The characteristics of the experimental rats are shown in table 1. The values of body weight and serum IRI were significantly greater in OLETF rats than in LETO rats at 12 weeks of age. However, no significant differences were found in blood glucose levels between the two strains. At the age of 30 and 39 weeks, blood glucose levels, body weights and values of IRI were significantly higher in OLETF rats than in LETO rats. Albuminuria was prominent in OLETF rats at these ages. There were no differences between the two strains in the ratio of kidney weight to body weight at each age experimented.

*Light Microscopy*

PAS and hematoxylin staining revealed a normal appearance of the renal tissue from LETO (fig. 1A) and OLETF (fig. 1B) rats at 12 weeks of age. At 30 weeks of age, a significant increase in the mesangial matrices was found in the glomerulus of OLETF rats (fig. 1D). No histological abnormalities were observed in the kidneys of age-matched LETO rats (fig. 1C).

*Immunofluorescence Staining*

We examined immunoreactivities for TGF-β, fibronectin and Smad2 in the glomeruli of rats aged 12 and 30 weeks. No differences were observed in the fluorescence intensity for TGF-$\beta_1$, fibronectin and Smad2 immunostaining in glomeruli between the two strains at 12 weeks of age (data not shown). At the age of 30 weeks, the TGF-$\beta_1$ immunostaining in glomeruli was more intense in OLETF rats (fig. 2B) than in LETO rats (fig. 2A). Non-

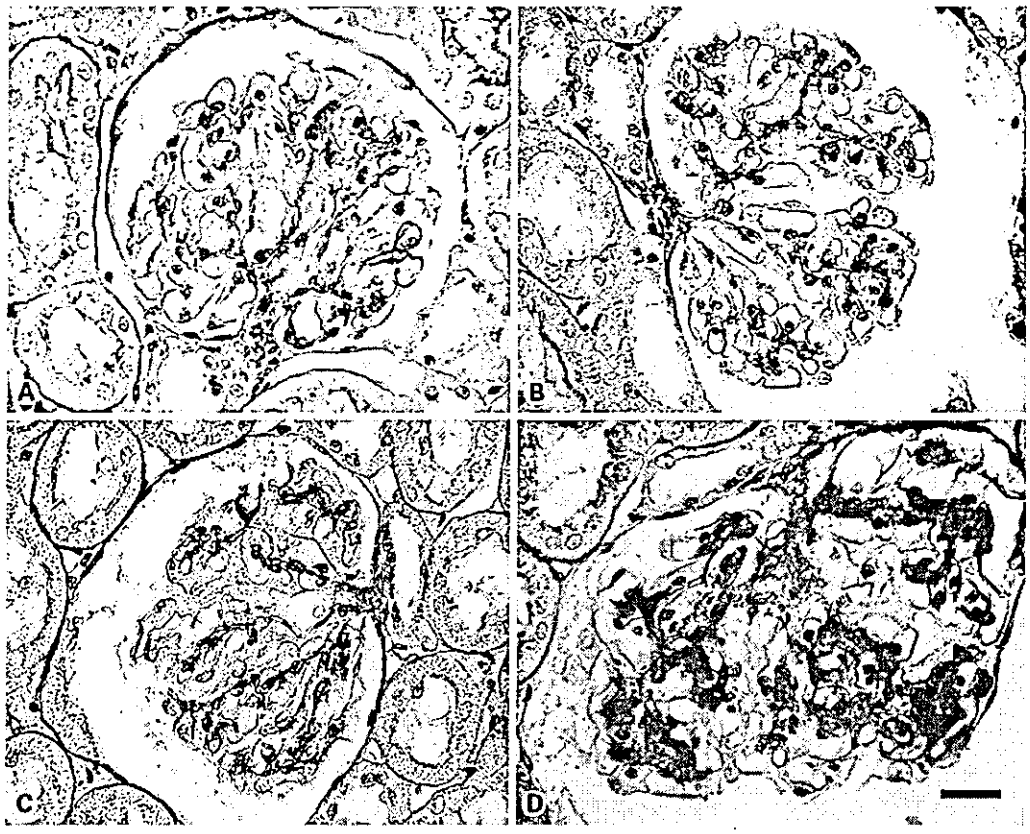


**Fig. 1.** Light micrographs of glomeruli from LETO (**A**, **C**) and OLETF (**B**, **D**) rats at the age of 12 weeks (**A**, **B**) and 30 weeks (**C**, **D**) stained with PAS and hematoxylin. Note the remarkable increase in the mesangial matrix in the glomerulus of OLETF rats at 30 weeks of age (**D**). Bar: 20 μm.

**Table 1.** Characteristics of the rats studied

| | n | Body weight, g | Kidney weight, mg | Kidney weight/body weight, mg/g | Fed blood glucose mg/dl | Urinary albumin mg/dl | IRI mg/dl |
|---|---|---|---|---|---|---|---|
| 12 weeks | | | | | | | |
| LETO | 6 | 351.7±6.0 | 1,689±75 | 4.65±0.22 | 174.3±15.9 | 0.8±0.2 | 1.5±0.3 |
| OLETF | 5 | 422.0±15.0** | 1,753±117 | 5.25±0.24 | 204.2±19.9 | 2.3±0.8 | 3.7±0.3** |
| 30 weeks | | | | | | | |
| LETO | 11 | 500.9±7.6 | 1,341± 84 | 2.98±0.17 | 171.0±10.2 | 3.9±2.6 | 2.7±0.9 |
| OLETF | 12 | 655.8±6.7*** | 1,831±90* | 2.98±0.13 | 299.2±18.1** | 227.9±51.5** | 7.2±0.8** |
| 39 weeks | | | | | | | |
| LETO | 4 | 510.0±10.8 | 1,659±59 | 3.25±0.09 | 139.5±10.9 | 6.1±2.1 | 1.1±0.4 |
| OLETF | 3 | 700.0±11.5* | 2,711±413* | 3.40±0.11 | 274.7±5.0* | 3,776.0±185.6* | 5.0±1.7* |

Data are means ± SE. * $p < 0.05$ vs. LETO; ** $p < 0.01$ vs. LETO; *** $p < 0.0001$ vs. LETO.

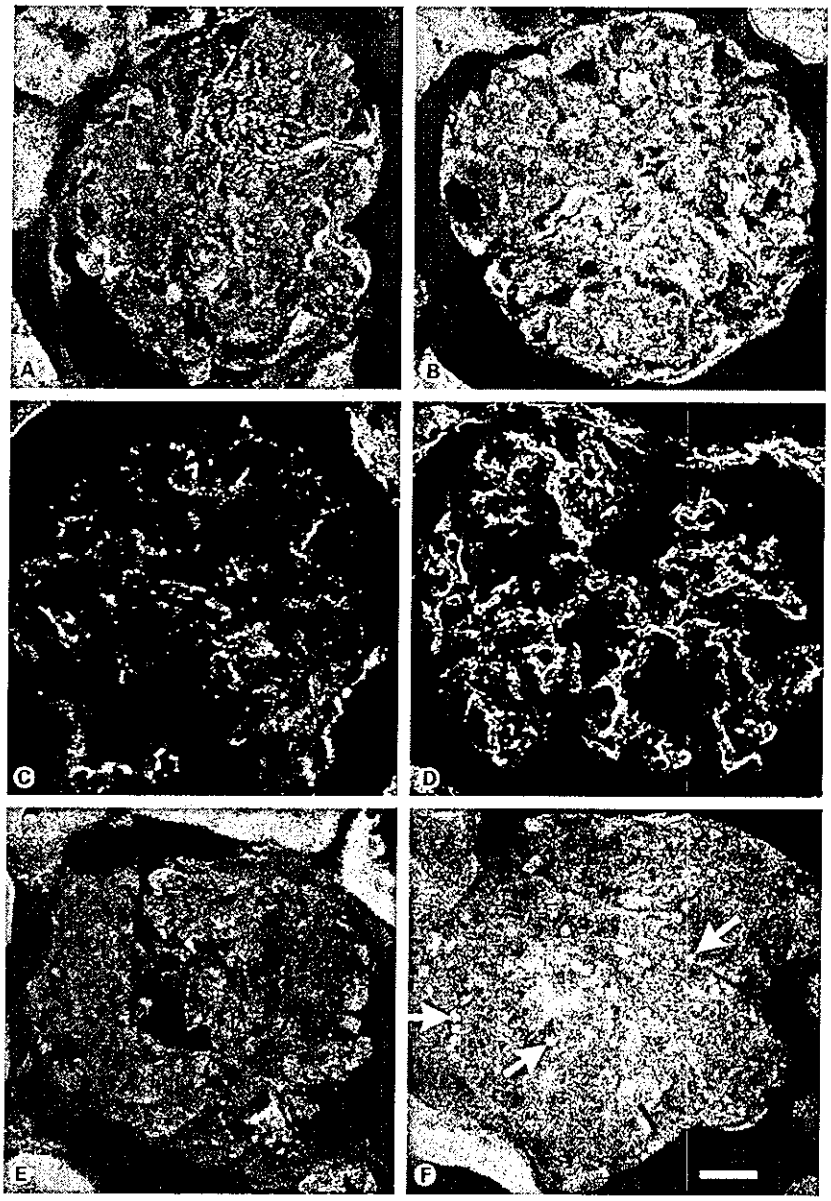


**Fig. 2.** Glomerular expression of TGF-$\beta_1$, fibronectin, and Smad2 proteins by immunofluorescence study. Immunofluorescence micrographs of glomeruli from LETO (**A**, **C**, **E** ) and OLETF (**B**, **D**, **F**) rats at 30 weeks of age stained for TGF-$\beta_1$ (**A**, **B**), fibronectin (**C**, **D**) and Smad2 (**E**, **F**) Intense immunostaining for TGF-$\beta_1$ was found in the glomeruli from OLETF rats (**B**) compared with LETO rats (**A**). The accumulation of fibronectin was evident in the mesangial areas in OLETF rats (**D**), while much less was found in LETO rats (**C**). The immunoreactivity for Smad2 was more intense in the glomeruli of OLETF rats (**F**) than in those of LETO rats (**E**). Arrows indicate strong immunopositive reactions for Smad2 in the nuclei of the glomerular cells from OLETF rats (**F**). Bar: 20 μm.

specific staining was observed in renal tubules as previously reported by Isaka et al [24]. Intense staining for fibronectin was observed in the mesangial areas in the glomerulus of OLETF rats (fig. 2D). The staining was more striking than those of LETO rats (fig. 2C). The immunoreactivity for Smad2, which is the mediator of TGF-β signal transduction, was more intense in the glomeruli from OLETF rats compared with LETO rats (fig. 2E). Furthermore, the strong immunopositive reactions for Smad2 were found to localize in the nuclei of the glomerular cells from OLETF rats (fig. 2F). The sections stained by methods eliminating incubation with primary antibodies showed only trace staining in glomeruli (data not shown). Expression of these proteins in glomeruli was quantified as described in the Methods section. The protein expression of TGF-$\beta_1$ (fig. 3A), fibronectin (fig. 3B) and Smad2